



# The Impact of Hole Geometry on the Near-wellbore Stress Around a Damage Wellbore

Ngurah Beni Setiawan

Imperial College London, UK  
Email: [nbenisetiawan@outlook.com](mailto:nbenisetiawan@outlook.com)

---

**Abstract.** In petroleum drilling, it has been observed that the actual wellbore is always deteriorated from ideal circular geometry. It is widely known that the standard stress calculation method is limited to a wellbore with a circular cross-section, and hence can no longer be used. In many practical oilfield operations, such as post-drill open hole stability assessment and hydraulic fracturing, information regarding the near-wellbore stress state after the wellbore has been drilled may still be required. Recently, Setiawan and Zimmerman (2020) proposed a semi-analytical method for the calculation of the stresses around a wellbore having an essentially arbitrary cross-sectional shape. To examine the significance of hole geometry on the near-wellbore stress, an actual wellbore has been reconstructed from an ultrasonic log. The in-plane near-wellbore stress is computed from the known hole geometry in a given *in situ* stress to identify zones of high-stress concentration attributed to the local irregularities around the wellbore. It is found that irregularity of the hole geometry has a significant impact on the near-wellbore stress. The stress concentration around such an irregular cross-sectional wellbore could be up to 50% higher than that of the standard computation. The impact of such under-estimation could be significant in various operations such as hydraulic fracturing, cementing, completion and perforation, where knowledge about the near-wellbore stress is crucial. Hence, the current method provides accurate near-wellbore stress without taking any assumption regarding the wellbore geometry.

**Keyword:** Wellbore stability; Non-circular hole.

---

©2020 IATMI. All rights reserved.

## 1 Introduction

In many practical oilfield operations, such as post-drill open hole stability assessment and hydraulic fracturing, information regarding the near-wellbore stress state after the wellbore has been drilled may still be required. It has been observed that the actual wellbore is always deteriorated from ideal circular geometry after the excavation. The standard stress calculation method such as the Kirsch solution is limited to a wellbore with a circular cross-section, and hence can no longer be used.

The shear failure around the wellbore occurs in response to the high-stress concentration due to stress redistribution after the excavation. Other factors such as drill string vibration, unconsolidated formation, hydraulic erosion, time-dependent chemical arise from the interaction between the drilling fluid with the



rocks, could worsen the already over gauge hole and further deteriorates the wellbore shape from circular to completely irregular. Hence, a solution for the stress calculation that accounts for such irregularity is needed.

Recently, Setiawan and Zimmerman (2020) proposed a semi-analytical method for the calculation of the stresses around a wellbore having an essentially arbitrary cross-sectional shape. Unlike traditional methods such as Kirsch's equation, the proposed semi-analytical solution allows the calculation of the stress components around the wellbore wall even after the wellbore has been damaged; hence allowing a more accurate assessment of the stability post drilling. This semi-analytical method only requires the outline coordinate of the hole and the elastic property of the material.

This paper presents an analysis to evaluate the impact of the wellbore cross-sectional irregularities on the near-wellbore stress. To examine the significance of hole geometry on the near-wellbore stress, an actual wellbore has been reconstructed from ultrasonic data. The in-plane near-wellbore stress is then computed from the known hole geometry in a given *in situ* stress to identify zones of high-stress concentration attributed to the local irregularities around the wellbore.

## 2 Stress around irregular cross-sectional holes

Setiawan and Zimmerman (2020) proposed a unified semi-analytical method to compute the stress around an irregular cross-sectional shape. The method can also take into account the anisotropic elasticity of the material. Unlike the traditional stress computation commonly used in petroleum application, *i.e.* a method that is limited for isotropic material and circular openings, the proposed method provides flexibility in terms of material characteristic and, most importantly, hole geometry. The elastic intrinsic behaviour of the rocks is characterised by the two roots of material characteristic  $\mathbb{Q}_\alpha$  ( $\alpha = 1, 2$ ). By taking the two roots to be nearly equal, the solution can be used for isotropic materials (Setiawan and Zimmerman, 2020). There are two elements of computation in the proposed methods: (1) conformal mapping using the Melentiev's successive approximation and (2) stress computation using the Kolosov-Muskhelishvili complex potential. Setiawan and Zimmerman (2020) provide the detail derivation of the method which will only be briefly repeated in this paper.

### 2.1 Conformal mapping

To start the computation, it is necessary to first transform the geometry of the physical hole in  $\mathbb{R}$ -plane into another domain in  $\mathbb{R}$ -plane, as such the geometry can be represented by a unit circle. By conformally mapping the physical hole, which can be in any kind of shape, into a unit circle, the mathematical solution can be easily obtained in the second domain. Numerous researchers have proposed analytical expressions for a range of geometry such as elliptical hole, rectangles, squares, ovals or quasi-triangles (see for instance Savin (1961); Lekhnitskii (1968); Daoust & Hoa (1991); Greenspan (1944)), but for petroleum application, a general method is needed to produce an adequate conformal mapping of an irregular hole shape that cannot be described by a simple analytical expression, such as borehole breakout or washout.



For this purpose, the method used the graphical method proposed by Melentiev (Melentiev, 1937; Kantorovich and Krylov, 1958). The following relation for the conformal mapping is considered:

$$\omega = \omega(\omega) = \sum_{k=0}^{\infty} \alpha_k \omega^{1-k} = \alpha_0 \omega + \alpha_1 + \alpha_2 \omega^{-1} + \dots \quad (1)$$

where the constant  $\alpha_k = \alpha_k + \alpha_k \omega_k$  must be determined to conformally maps the external region in the  $\omega$ -plane into the external region of the unit circle in  $\omega$ -plane. An iterative process is required to determine the most appropriate values of the coefficients  $\alpha_k$  and  $\beta_k$  such that the approximated contour is as close as possible to the desired contour in the  $z$ -plane (see Figure 1). To achieve this, as illustrated in Figure 1, a line is drawn from the point  $M_n^{(0)}$  to the origin, and the intersection of this line with the curve  $L$  is taken to be the new point  $M_n^{(1)}$ . The ray  $O-M_n^{(1)}$  is then projected onto the ray  $O-u_n^{(0)}$  which will be the initial step in the iteration. The process will have to be done for all known outline coordinate of the wellbore.

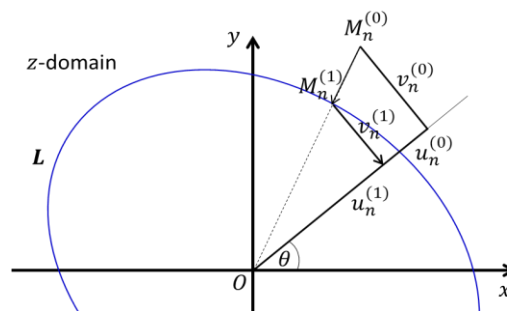


Figure 1. A step in the iterative procedure to transfer point  $M_n^{(0)}$  to the contour  $L$ .

Figure 2 shows an example of the region outside a triangle conformally mapped into the region outside the unit circle. The closed curves and quasi-radial lines in the  $z$ -plane correspond to constant values of the angular and radial coordinates in the  $\xi$ -plane. The orthogonality of these curves in the  $z$ -plane shows that the mapping is indeed conformal.

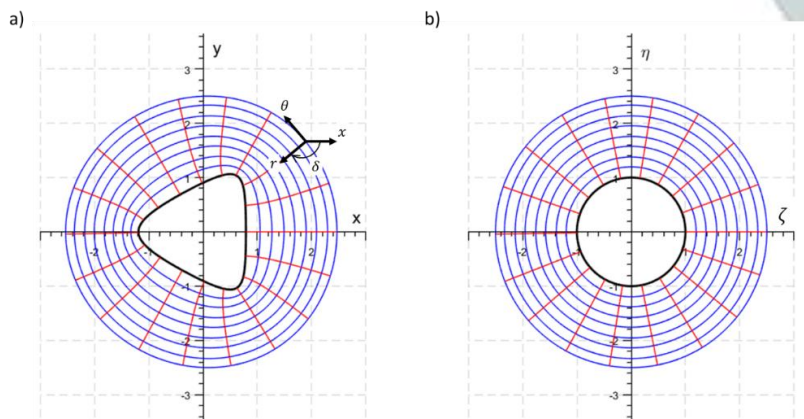


Figure 2. Conformal mapping of the region outside a triangular shape in (a) the  $z$ -plane into the region outside the unit circle in (b) the  $\xi$ -plane.



## 2.2 Formulation of the complex potentials

The in-plane stress components can be computed from the derivative of two complex potentials, *i.e.*  $\varphi'_0(\varpi_1)$  and  $\psi'_0(\varpi_2)$ , given by

$$\begin{aligned}\varpi_{\varpi\varpi} &= \varpi_{\varpi\varpi}^{\infty} + 2\varpi\varpi[\varpi_1^2\varpi'_0(\varpi_1) + \varpi_2^2\varpi'_0(\varpi_2)] \\ \varpi_{\varpi\varpi} &= \varpi_{\varpi\varpi}^{\infty} + 2\varpi\varpi[\varpi'_0(\varpi_1) + \varpi'_0(\varpi_2)] \\ \varpi_{\varpi\varpi} &= \varpi_{\varpi\varpi}^{\infty} - 2\varpi\varpi[\varpi_1\varpi'_0(\varpi_1) + \varpi_2\varpi'_0(\varpi_2)]\end{aligned}\quad (2)$$

in which  $\varpi_{\varpi\varpi}^{\infty}$ ,  $\varpi_{\varpi\varpi}^{\infty}$  and  $\varpi_{\varpi\varpi}^{\infty}$  are the applied (far-field) *in situ* stresses and  $\varpi_{\varpi}$  ( $\varpi = 1, 2$ ) is the root of the material characteristic equation and is related to the elastic moduli of the rock. In the  $\xi$ -plane, the two complex potentials are:

$$\begin{aligned}\phi_0(\xi) &= A_1\alpha_0\xi^{-1} + A_2\beta_0\xi^{-1} + A_3\sum_{k=2}^N\alpha_k\xi^{1-k} + A_4\sum_{k=2}^N\beta_k\xi^{1-k} \\ \psi_0(\xi) &= A_5\alpha_0\xi^{-1} + A_6\beta_0\xi^{-1} + A_7\sum_{k=2}^N\alpha_k\xi^{1-k} + A_8\sum_{k=2}^N\beta_k\xi^{1-k}\end{aligned}\quad (3)$$

where  $A_i$  ( $i = 1 \dots 8$ ) depends on the material characteristic and far-field stress (Setiawan and Zimmerman, 2020).

## 3 Result and discussion

To substantiate the analysis, a total of 180 data points was obtained at each depth from the ultrasonic borehole imaging data; this will give a  $2^\circ$  azimuthal resolution of wellbore circumference that can sufficiently capture any local irregularities around the wellbore wall. The profile of the wellbore is shown in Figure 3. The middle plot in the figure shows the cross-sectional wellbore from the top of the wellbore to the bottom. At several depths, it seems that the hole size is less than the bit-size (black circle) which seems to be due to the quality of the measurement and processing. The last track in Figure 3 also shows a severely damaged wellbore throughout the wellbore. The actual bit size over this interval is 8.5 inch which gives a radius of 4.25 inch. However, as seen in the plot the area of enlargement is between 25% to nearly 50% of an ideal wellbore; indicating the severity of the wellbore damage. Stress computation using a traditional approach would certainly produce an erroneous result.

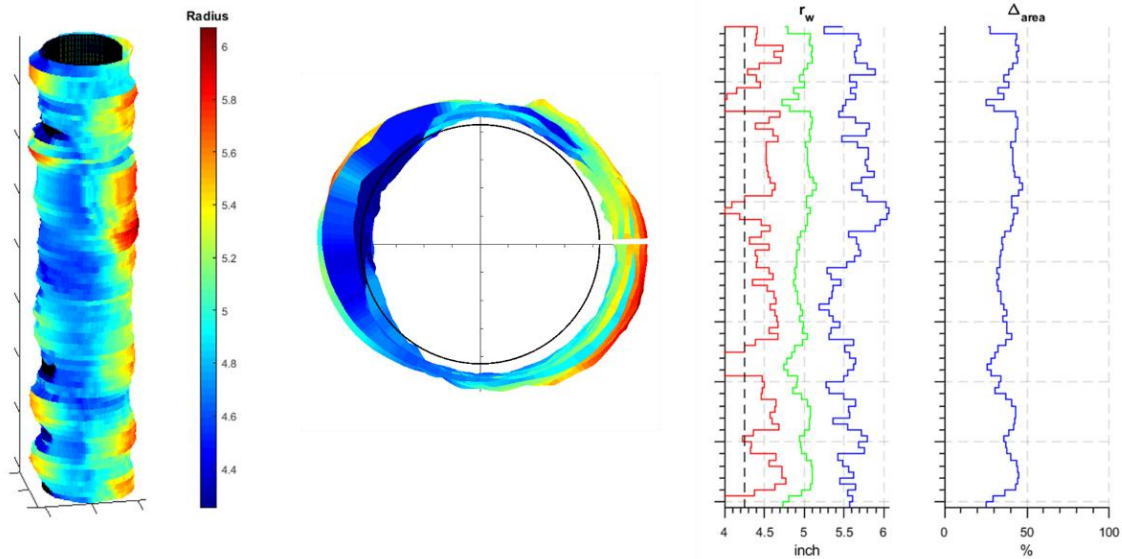


Figure 3. The hole shape showing the irregularities of the cross-section. The wellbore was drilled with an 8.5 inch drill-bit (4.25 inch radius).

The amount of computation time for each depth with 180 data points is less a second, which, in this work was run using a laptop DELL Inspiron 5459 Intel i5-6200U with 8GB RAM. The wellbore geometry shown in Figure 3 is taken from A dataset from the *Western Australian Petroleum and Geothermal Information Management System* (WAPIMS). The WAPIMS provides released data and all public information arising out of petroleum exploration activities within Western Australia's State jurisdiction (onshore and State territorial waters) together with Commonwealth offshore activities released prior to 1 January 2012.

To demonstrate the impact of wellbore geometry on the in-plane stress computation, the following assumption is made regarding the *in situ* stress around the wellbore: the vertical *in situ* stress ( $\sigma_v$ ) is assumed to be 10,000 psi with 7,000 and 9,000 psi for minimum ( $\sigma_h$ ) and maximum ( $\sigma_H$ ) horizontal stresses, respectively. The azimuth of the minimum horizontal stress is parallel with the North. Figure 4 shows the cross-sectional at one particular depth from the wellbore. (It is worth noting that a proper geomechanical analysis should be done to obtain the *in situ* stress magnitude which was not done in the present analysis for the respective dataset.)

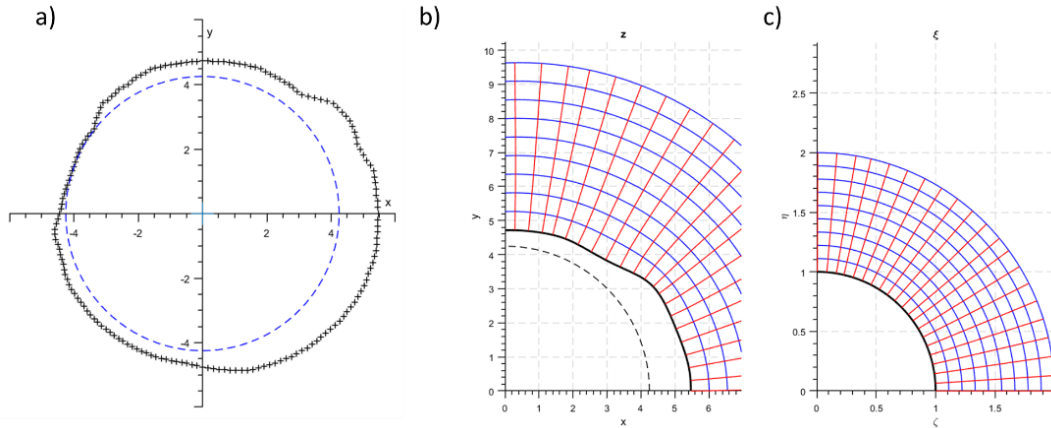


Figure 4. (a) Actual wellbore showing the cross-sectional irregularities reconstructed using 180 points from the ultrasonic data. (b) The orthogonality of the closed curves and quasi-radial lines in the  $z$ -plane correspond to constant values of the angular and radial coordinates in (c) the  $\xi$ -plane; indicating the mapping is indeed conformal.

The Melentiev's successive approximation is then used to determine the conformal mapping constant to produce a profile shown in Figure 4b; but only the top quarter of the hole is shown here. It is obvious from Figure 4b that the orthogonality of the quasi-radial line and the closed curve is maintained. The stress components can now be computed using the new representation of the complex potential proposed by Setiawan and Zimmerman (2020) as in Eq. 3. The stress components given in Eq. 2 can be transformed into tangential stress  $\sigma_\theta$  to quantify the amount of stress concentration around the wellbore, using the following equations:

$$\begin{aligned}\sigma_{\theta\theta} - \sigma_{rr} + 2\sigma_{r\theta} &= (\sigma_{xx} - \sigma_{yy} + 2\sigma_{xy})e^{2i\delta} \\ \sigma_{\theta\theta} + \sigma_{rr} &= \sigma_{xx} + \sigma_{yy}\end{aligned}\quad (4)$$

in which  $\delta$  is the rotational angle from the  $x$ -axis to the radial axis  $r$  (see Figure 2). For biaxial tension or compression, the principle of superposition can be used.

The tangential stress  $\sigma_\theta$  of the wellbore is shown in Figure 5; in which the left plot is from the actual wellbore shape and the one on the right is computed assuming a circular wellbore. Two things can be observed in here: (1) the location of the stress concentration is shifted and affected by the curvature of the hole geometry and (2) the magnitude of the stress concentration is also substantially different. The concentrated stress that is supposed to be located at the top of the wellbore with a magnitude of 20,000 psi if the wellbore is assumed to be a circle, is now localised at, at least, two different locations with a magnitude of approximately 10% higher. Moreover, at several locations around the wellbore, the tangential stress seems to be relaxing as shown by a relatively darker blue colour as compared to that of the circular wellbore. These findings emphasize the impact of hole geometry on the near-wellbore stress and how inaccurate near-wellbore stress computation could be avoided using a more robust approach presented here.

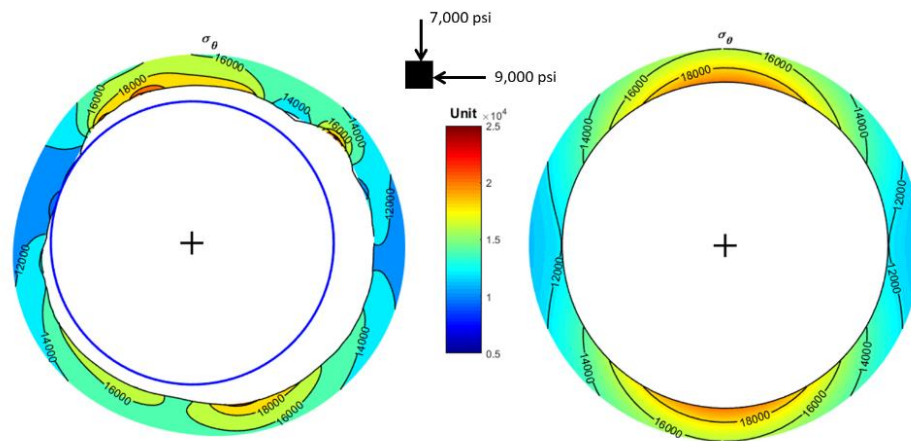


Figure 5. The tangential stress around the wellbore using the actual wellbore geometry (left) and a circular wellbore. The concentrated stress is shifted and the magnitude of the stress is substantially different between the two cases; indicating the impact of wellbore geometry on the stress computation.

If the same process is repeated along the wellbore, the tangential stress throughout the wellbore can be obtained. Perhaps, the most interesting question to ask is how significant is the impact of the hole geometry on the stress concentration. To illustrate its significance, the percentage difference of the minimum and maximum tangential stress at each depth with that of the Kirsch solution is calculated; as shown in Figure 6. Throughout the hole section, particularly at the top half of the wellbore, the maximum tangential stress (the red curve) is approximately 30% higher than that of the standard calculation. The minimum horizontal stress, shown as the blue curve, indicates that a magnitude of nearly 50% less than that from the Kirsch solution is expected halfway to the bottom of the wellbore. The direct conclusion of these findings is obvious in that one must compute the stress component using a method that acknowledges the geometry of the wellbore. Perforation, completion and hydraulic fracturing design may still require information regarding the stress distribution around the wellbore. Hence, a more robust method must be used to compute the stress to ensure an accurate result can be obtained.

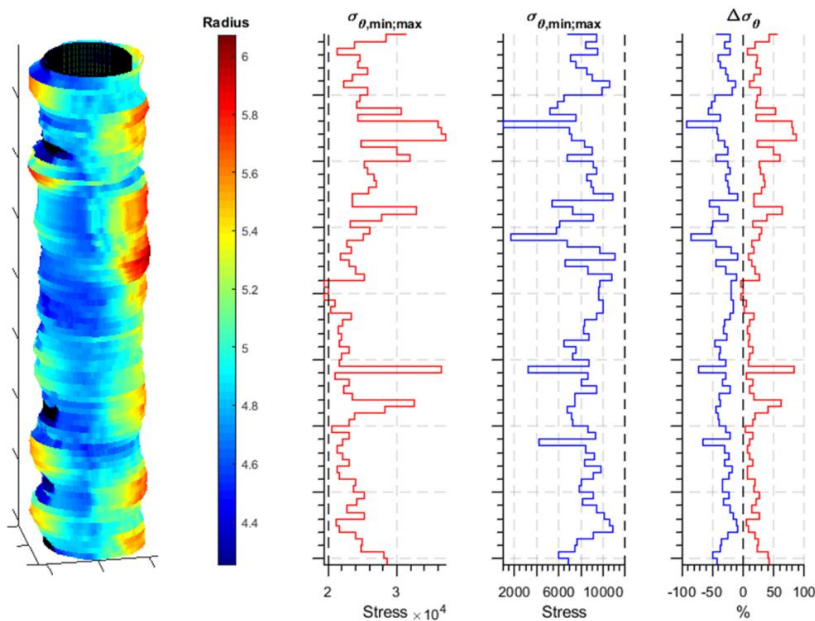


Figure 6. The tangential stress around the wellbore. The red curve shows the maximum tangential stress and the blue curve is for the minimum tangential stress. The percentage difference with that of the Kirch solution is shown in the last track.

#### 4 Conclusion

This paper presents a discussion about the importance of acknowledging the actual wellbore geometry in computing the in-plane stress for many petroleum engineering designs. Wellbore geometry affects the distribution of the near-wellbore stress in two ways, as shown in this paper; the first one is the shifting of the concentrated stress at the wellbore wall and also the substantial increase (and decrease) of the stress magnitude. For the case considered here, the maximum and minimum tangential stress could reach 30% to 50% different from that of the traditional approach. The impact of such under-estimation (or over-estimation) could be significant in various operations such as hydraulic fracturing, cementing, and perforation, where knowledge about the near-wellbore stress are crucial.

#### Acknowledgement

The author would like to thank Sonny Wiyoga of Schlumberger Jakarta for the discussion regarding the ultrasonic borehole imaging and wellbore geometry reconstruction.

#### References

- [1] Greenspan, M. (1944). Effect of a Small Hole on the Stresses in a Uniformly Loaded Plate. *Quarterly of Applied Mathematics*, 2(1), 60–71.
- [2] Kantorovich, L. V, & Krylov, V. I. (1958). *Approximate Methods of Higher Analysis*. Noordhoff, Groningen.



- [3] Lekhnitskii, S. G. (1968). *Anisotropic Plates*. Gordon and Breach, New York.
- [4] Melentiev, P. V. (1937). *Several New Methods and Devices for Approximate Computations*. Moscow-Leningrad.
- [5] Savin, G. N. (1961). *Stress concentration around holes*. Pergamon Press.
- [6] Setiawan, N. B., & Zimmerman, R. W. (2020). A Unified Methodology for Computing the Stresses around an Arbitrarily-Shaped Hole in Isotropic or Anisotropic Materials. *International Journal of Solids and Structures*, 199, 131–143.